A Modified Model to Determine Heat Generation in the Friction Stir Welding Process

A. Ghiasvand [*], S. Hassanifard, M. Zehsaz

Department of Mechanical Engineering, University of Tabriz, Tabriz, Iran

ABSTRACT

Friction stir welding (FSW) is a solid state bonding process in which the parts are joined together at the temperature below the melting point. In present study, a modified model was developed based on the partial sticking/sliding assumption in the tool-work piece interface and the dependence of the thermal energy equations on the temperature-dependent yield stress to determine heat generation in FSW process that is independent from coefficient of friction. So to eliminate the dependence of the final equations on the coefficient of friction, an equation was used which the coefficient of friction was expressed as a function of work piece yield stress. To validate the model, the FSW process was simulated by the finite element package ABAQUS and two subroutines of DFLUX and USDFLD and then the simulation results were compared with the experimental ones. The results showed that the modified model is appropriately capable of predicting the temperature and the residual stresses in the different zones of welded section.

© 2021 IAU, Arak Branch. All rights reserved.

Keywords: Friction stir welding; Thermal model; Coefficient of friction; Yield stress; Numerical simulation.

1 INTRODUCTION

FRICTION stir welding (FSW) was first invented at The Welding Institute (TWI) in the UK in 1991 [1]. Compared to other welding methods, FSW offers several advantages such as less residual stress, fine microstructure, less required input energy, and improved mechanical quality of the joint [2]. Due to the anti-symmetry nature of the FSW process, two distinct zones (advancing side and retreating side) are formed with different microstructures and mechanical characteristics on either sides of the joint line [3]. The weld cross section in the FSW process is divided into three main sections: sections of stir zone (SZ), thermo-mechanically affected zone (TMAZ), and the heat-affected zone (HAZ). The heat distribution conditions and the different plastic strains in these three regions cause these three zones to have major differences in microstructural and mechanical properties. Hence, the modeling of the heat distribution in different welding regions leads to a more accurate prediction of the temperature distribution in the work piece and the final joint properties, ultimately leading to the establishment of an improved quality bonding. Due to a lack of an efficient analytical model as well as the cost and limitation of

_____
[*]Corresponding author. Tel.: +98 4133392467.
E-mail address: Amir.Ghiasvand@tabrizu.ac.ir (A. Ghiasvand)

experimental conditions, it seems necessary to develop new models and study their analytical relationships in order to predict thermal conditions in the FSW process. Some researchers have investigated and modeled heat generation in the FSW process analytically and numerically. For example, Frigaard et al. [4] presented a model of heat generation based on the friction and constant friction coefficient. The model was then analyzed in a three-dimensional manner through the use of finite difference method. The researchers observed that the heat source in FSW is symmetrical and the same temperature lines around the plastic deformed area reach an average temperature of 450 Celsius. To determine the amount of heat generated in the process, they used a common model of heat generation and chose a friction coefficient equal to 0.4 to take into account the heat generated by the plastic work. Chao et al. [5] also used a three-dimensional finite element model assuming that all of the generated heat is owing to the friction between tool and work piece. The generated heat was also assumed to be distributed radially in the top surface of the work piece. To predict the heat distribution in the work piece, Chao et al. used a thermal model in which the friction coefficient was assumed to be constant. Chen and Kovacevic [6] aimed to create a three-dimensional finite element model in order to estimate and predict heat generation and thermal field in the work piece. In their study, the heat generated by shoulder was regarded as the single factor and the heat generated by the tool pins and the amount of heat absorbed by the tool were neglected. Khandkar et al. [7] offered a thermal model in which the heat generation in the FSW process was modeled based on the experimentally-measured torque distribution. Song and Kovacevic [8] developed a model based on a moving heat source in order to predict the heat generated in the work piece. In their investigation, both sources of the generated heat by tool pin and tool shoulder were considered. In the equations developed by Song and Kovacevic, the values of friction coefficient and shear yield stress were considered constant and final equations were solved using the finite difference method. Schmidt et al. [9] presented an analytical method for investigation of heat generated in friction stir welding of AA2024 Aluminum alloy. In their research, frictional conditions between tool and work piece were modeled using sticking and sliding conditions. The researchers considered the interaction conditions between tool and work piece as three forms of full sliding, full sticking and partial sticking/sliding. In this study, friction model was divided and categorized into three different sections between tool and work piece. In all these three sections, shear yielding stress and friction coefficient were considered as a constant value. Nandan et al. [10] studied heat transfer and plastic material flow in the FSW process of mild steel due to a three dimensional temperature-displacement coupling model. The results showed that by increasing rotational speed, the plastic flow as well as the generated heat increases. Schmidt and Hattel [11] applied a three-dimensional finite element model to investigate temperature distribution and material flow in the FSW process using Arbitrary Lagrangian–Eulerian (ALE) technique, Johnson-Cook equation, and a constant friction coefficient. Riahi and Nazari [12] studied the heat distribution in FSW of AA6061 Aluminum alloy. The researchers considered tool pin and tool shoulder as the main heat generation sources. Although numerous models have been introduced in the literature to model heat generation in the FSW process, there exists no precise and comprehensive thermal model to predict heat and temperature distribution, microstructure changes, and other mechanical properties. One reason for this might be paying inadequate attention to potential factors involved in the process or assuming that some important parameters of the process are constant.

In many of the researches on heat generation, various factors including friction coefficient, shear yield stress, plunge depth, tool pin geometry, and the applied force by tool and modeling of the all of thermal sources are not simultaneously taken into consideration. Accordingly, the current research aims to develop a model independent from friction coefficient using analytical relations. To validate the model, a three-dimensional finite element simulation is used by ABAQUS package with two subroutines of DFLUX, USDFLD. Finally, the results of temperature distribution obtained from the developed model are compared with the experimental results.

2   HEAT GENERATION MODEL

According to studies conducted in the area of heat generation, researchers maintain that a large portion of the generated heat (from 80 to 98%) in the FSW process is due to the friction between the tool and the work piece. However, most of the energy derived from plastic deformation is stored in microstructure of the welding regions [13, 14]. Thus, in the present study, only the heat generated by friction and interaction between the engaged surfaces were examined, neglecting the heat generated by plastic flow of material.

After plunging the tool in work piece, three different contact zones between the tool and work piece are created, each of which can produce a portion of the generated heat of the process. The first zone, introduced by Q_1, belongs to the heat generated due to the interaction and friction between tool shoulder surface and upper surface of work piece. The second zone produces the energy of Q_2 and this heat source is created by interaction and friction between

tool pin wall and work piece material surrounding the pin. The third zone belongs to the thermal energy of Q_3 and this source is produced as a result of the contact between pin tip and work piece. The schematic structure of these three heat generation sources is represented in Fig. 1.
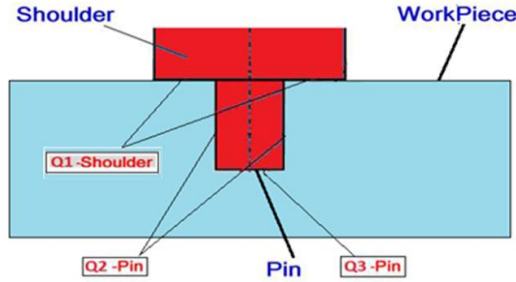
Fig.1
Heat generation sources in FSW process.

Due to the assumption of neglecting the heat generated from plastic work, the thermal input energy of the process can be expressed as Eq. (1). This thermal input energy originates from two factors of pin and tool shoulder and the portion of each factor can be considered as Eq. (3) and Eq. (4).

$$Q_{FSW} = Q_1 + Q_2 + Q_3 \tag{1}$$

$$Q_{FSW} = Q_{shoulder} + Q_{pin} \tag{2}$$

$$Q_{shoulder} = Q_1 \tag{3}$$

$$Q_{pin} = Q_1 + Q_2 \tag{4}$$

According to Schmidt's model of heat generation [9], for a tool with conical shoulder and a simple cylindrical pin, the heat is generated by contact and interaction among three surfaces and the value of these three heat sources can be calculated as following equations:

$$Q_1 = \frac{2}{3} \pi \tau_{shear} \omega \left(R_{shoulder}^3 - R_{pin}^3 \right) (1 - \tan \alpha) \tag{5}$$

$$Q_2 = 2 \pi \tau_{shear} R_{pin}^2 H_{pin} \omega \tag{6}$$

$$Q_3 = \frac{2}{3} \pi \tau_{shear} R_{pin}^3 \omega \tag{7}$$

where R_{pin}, $R_{shoulder}$, ω, H_{pin}, α and τ_{shear} are pin radius, shoulder radius, tools angular rotation speed, pin height, shoulder conical angle (if conical shoulder is used), and shear stress created in each of the triple zones respectively. According to Eq. (5) to Eq. (7), the total heat generated in the FSW process is equal to:

$$Q_{FSW} = \frac{2}{3} \pi \tau_{shear} \omega [(R_{Shoulder}^3 - R_{Pin}^3)(1 + \tan \alpha) + R_{Pin}^3 + 3 R_{Pin}^2 H_{Pin}] \tag{8}$$

All of the parameters in Eq. (8) are constant in the cycle of process except τ_{shear}. Based on the available thermal models, two different approaches have been used to calculate τ_{shear} in the FSW process. Some models assume that frictional condition is full sticking in the tool-work piece interface and τ_{shear} is then considered as a constant value equal to Eq. (9). Based on this, the total input heat is calculated as Eq. (10).

$$\tau_{shear} = \frac{\sigma_{yield}}{\sqrt{3}} \tag{9}$$

$$Q_{FSW\,(Sticking)} = \frac{2}{3}\pi\omega\frac{\sigma_{yield}}{\sqrt{3}}((R_{Shoulder}^3 - R_{Pin}^3)(1+\tan\alpha)+R_{Pin}^3+3R_{Pin}^2H_{Pin}) \tag{10}$$

where σ_{yield} is the yield stress of the work piece material. Similarly, some models assume that frictional condition is full sliding in the tool-work piece interface and in these models τ_{shear} is expressed as a constant value and a function of three parameters of friction coefficient μ, total area A_{Totlal} and the applied force by the tool F_z. According to the full sliding condition assumption, the total generated heat is achieved as Eq. (13).

$$\tau_{shear} = \frac{\mu F_z}{A_{Total}} \tag{11}$$

$$A_{totlal} = \pi R_{shoulder}^2 \tag{12}$$

$$Q_{FSW\,(Sliding)} = \frac{2}{3}\omega\mu\frac{F_z}{R_{shoulder}^2}((R_{Shoulder}^3 - R_{Pin}^3)(1+\tan\alpha)+R_{Pin}^3+3R_{Pin}^2H_{Pin}) \tag{13}$$

One of the common problems in the available thermal models of the FSW process is a lack of attention to the shear yield stress and the coefficient of friction because of the change in the process temperature (instantaneous and local temperature). Thus, in the available models, friction conditions are either full sliding or full sticking. However, considering the nature of the process, a hybrid, model dependent on the time and location of the tool-work piece interface, should be employed. According to recent researches, interface conditions in frictions zones of Q_1 and Q_2 are full sticking due to high temperature and heat concentration in these zones and in Q_3 zone which belongs to the contact area between pin bottom and work piece is sliding because of great distance from shoulder, which is the main reason for heat generation, and lower temperature in this zone. On other hand, in the FSW process, the yield stress and the coefficient of friction are strongly dependent on temperature variations, and these two parameters must also be defined as field and temperature-dependent variables. In order to remove the above-mentioned deficiencies, in the present study a combined model of sliding and sticking dependent on the instantaneous temperature of the process is used. Therefore, new relation is written with the assumption of the dependence of the shear yield stresses of triple zones and the coefficient of friction on the local and instantaneous temperatures:

$$\tau_{shear}(Q_1) = \frac{\sigma_{yield}(T)}{\sqrt{3}} \tag{14}$$

$$\tau_{shear}(Q_2) = \frac{\sigma_{yield}(T)}{\sqrt{3}} \tag{15}$$

$$\tau_{shear}(Q_3) = \frac{\mu(T)F_z}{A_{Bpin}} \tag{16}$$

where A_{Bpin} is the tool pin tip area. According to the nature of the process, the total heat generated during the process is absorbed partly by work piece and tool, and such absorbed heat increases the temperature of these two parts. In the current model, in order to investigate the portion of the absorbed heat by tool, a parameter named λ, is used varying between 0 and 1; 0 refers to the condition that no heat is transferred to work piece and 1 stands for a condition that all of the heat is absorbed by work piece.

In the available thermally based models, mainly a pin with cylindrical geometry whose radius is constant over the entire length of the pin has been used. While the use of taper cylindrical pin is widely used in the FSW process

[15, 16]. To solve this problem, the parameters of R_{Tpin} and R_{Bpin} are used to introduce the radius of the upper and lower radius of the pin respectively in the current model so that the effects of the tool pin geometry can be considered in the equation. By replacing Eq. (14) and Eq. (15) with Eq. (5) and Eq. (7), substeduding λ in the equations and defining new equations based on the taper cylindrical pin, thermal equations of the three different zones can be rewritten as:

$$Q_1 = \frac{2}{3}(T)\pi\lambda\omega\frac{\sigma_{yield}}{\sqrt{3}}(R_{shoulder}^3 - R_{Tpin}^3)(1 + \tan\alpha) \tag{17}$$

$$Q_2 = 2\pi\lambda\omega H_{pin}\frac{\sigma_{yield}(T)}{\sqrt{3}}(\frac{R_{Tpin} + R_{Bpin}}{2}) \tag{18}$$

$$Q_3 = \frac{2}{3}\pi\lambda\omega\mu(T)\frac{F_z}{A_{Bpin}}R_{Bpin}^2 \tag{19}$$

A major drawback associated with analytical models is using only one general surface heat flux (applied to the top surface of work piece) which leads to the lack of heat flow as a mixture of body and surface fluxes in the depth of the work piece. Lack of attention to this factor makes a great deal of difference between the distribution of heat through the depth of the work piece and the actual conditions, and the temperature at the top surface of the work piece experiences a larger growth. However, based on experimental studies, in the middle depths of the work piece, relatively large thermal cycles are generated and the temperature experiences a significant increase [2]. Therefore, in the present model, in order to remove such disadvantages, the heat source Q_1 was considered as a surface heat flux applied to the surface of the work piece. The geometric location of the distribution of this surface heat flux is the enclosed area between the two circles, which their radii are equal to the shoulder radius and tool pin radius respectively. Two other sources of Q_2 and Q_3 which are the thermal sources caused by tool pin are applied as a body heat flux in the enclosed area of the tool pin. By using these equations, the effects of geometry and the occupied volume by tool pin are considered as influential factors in the FSW process. This makes it possible to study the effects of different pin geometries on the value of the input heat and temperature distribution in welding section for different geometrical situations. According to the above-stated discussion, the equations of two thermal sources are given as Eq. (20) and Eq. (21) for applying two surface and body heat fluxes to work piece.

$$Q_{pin} = 2\pi\lambda\omega H_{pin}\frac{\sigma_{yield}(T)}{\sqrt{3}}(\frac{R_{Tpin} + R_{Bpin}}{2}) + \frac{2}{3}\pi\lambda\omega\mu(T)\frac{F_z}{A_{Bpin}}R_{Bpin}^2 \tag{20}$$

$$Q_{shoulder} = \frac{2}{3}\pi\lambda\omega\frac{\sigma_{yield}(T)}{\sqrt{3}}(R_{shoulder}^3 - R_{Tpin}^3)(1 + \tan\alpha) \tag{21}$$

Except two parameters of σ_{yield} and μ which are temperature-dependent, other parameters in Eq. (20) and Eq. (21) are constant. Now, equations can be rewritten by defining and using a new relationship to correlate the coefficient of friction with the instantaneous yield stress. Therefore, in order to define friction coefficient based on work piece yield stress in various points of welding section, an analytical model proposed by Meyghani et al. [17] was used. In their study, Meyghani et al. first presented an analytical equation to calculate friction coefficient based on shear yield stress, which stands as Eq. (22). They then calculated the value of temperature-dependent friction coefficient using this equation.

$$\mu = \frac{0.5\tau_1}{\left(1 - \frac{\tau_1(1 - 1.5\sin\beta)}{(1 - \sin\beta)\tau_y}\right)P_0(1 - \sin\beta)} \tag{22}$$

where τ_y, τ_1, P_0 and β are work piece shear yield stress, contact shear yield stress in pin wall, pressure applied to the bottom of the pin and angle between pin and shoulder respectively. Based upon the assumption presented in the current model that the slip conditions are dominant in the pin wall, two parameters τ_1 and τ_y can be considered equal and these two values are calculated based on the work piece yield stress and replaced in the equations. By applying this condition and replacing a proper relevancy with P_0, Eq. (22) can be rewritten as:

$$\mu(T) = \frac{A_{Bpin}\sigma_{yield}(T)}{\sqrt{3}F_z \sin\beta} \tag{23}$$

Using Eq. (23) and replacing it with Eq. (20), two final equations of heat generation by shoulder and pin can be given as Eq. (24) and Eq. (25).

$$Q_{pin} = 2\pi\lambda\omega H_{pin}\frac{\sigma_{yield}(T)}{\sqrt{3}}(\frac{R_{Tpin}+R_{Bpin}}{2}) + \frac{2}{3}\pi\lambda\omega\frac{\sigma_{yield}(T)}{\sqrt{3}\sin\beta}R_{Bpin}^2 \tag{24}$$

$$Q_{shoulder} = \frac{2}{3}\pi\lambda\omega\frac{\sigma_{yield}(T)}{\sqrt{3}}(R_{Shoulder}^3 - R_{Tpin}^3)(1+\tan\alpha) \tag{25}$$

Using these two final equations, the heat generated in the FSW process is achieved on the basis of tool geometry, process parameters, and the temperature-dependent yield stress. In addition, the dependence of the generated heat equations on the friction coefficient is eliminated.

3   MODEL VERIFICATION

In order to validate the developed model, a numerical simulation of the FSW process was utilized in the present study using finite element package of ABAQUS [18]. As a factor for validating the model, temperature results obtained from numerical simulation (based on the developed model) were compared with the experimental results obtained from the literature review. Experimental data such as tool geometry, process parameters and work piece, and tool materials were based on Aval et al.'s study [19]. Numerical simulation was performed according to the experimental condition addressed in their study.

Dimensions and material of the work piece were considered according to the mentioned experimental research. Therefore, the work piece with dimensions of 150×100×5 *mm* was used. The tool was a concave shoulder with α angle equal to 2 degrees, a radius of 20 *mm* with a taper cylindrical pin with β angle equal to 72.6 degrees, upper radius of 3 *mm* (radius in intersection with shoulder), tip radius of 1.5 *mm* and length of 4.8 *mm*. Rotational and linear speed of tool were considered as 840 *rpm* and 150 *mm/min* respectively. According to the definition of λ and lack of need for modeling the thermal changes of tool during the process, geometrical modeling of the tool was neglected. Based on the literature review [10, 20], λ was defined as 0.75. Using coding, the dimensional range of pins was used as input data of FORTRAN code in DFLUX subroutine in order to determine the surrounded volume by pin to apply body heat flux. For this purpose, the pin radius was coded as a function of the pin-length parameter in the subroutine. By using this relationship and the developed relations in the present model, the heat generated by the tool pin was applied as a function of time and location of different points. According to the model developed in this study, equations related to the input heat generated by tool pin (Eq. (24)) and heat generated by tool shoulder (Eq. (25)) were used to apply body and surface heat fluxes. Based on these, two heat fluxes were applied to the work piece: a surface heat flux corresponding to the heat produced by the shoulder using the Eq. (25) applied on the upper surface of the work piece, and a body heat flux corresponding to the heat generated by the tool pin using the Eq. (24) applied to the total volume of the work piece. In order to apply these two heat fluxes, USDFLD subroutine was used in such a way that the amount of heat fluxes can be defined dependent to location, time and instantaneous and local temperature. It should be noted that simulation of plunging and retreating of tool were neglected and only the step of creating the joint was investigated. Lastly, by linking the written code to the software, the numerical analysis was conducted. Table 1 shows temperature-dependent thermal properties and yield stress of AA6061-T6.

Table 1
Thermal and mechanical properties of AA6061. [19]

Temperature	Density	Thermal Conductivity	Heat Capacity	Yield Stress
$C°$	Kg/m^3	$W/m.°C$	$J/Kg.°C$	MPa
25		167	896	276
100		180	978	262
150		184	1004	214
200	2700	192	1028	103
250		201	1052	34
300		207	1078	19
450		230	1133	12

In order to apply the boundary conditions to the model, various convection heat transfer coefficients were used for different parts. Considering the lack of anvil modeling, a relatively huge virtual convection heat transfer coefficient was used for this section. In order to mesh the model, 10500 elements from DCC3D8 family were used. These elements are brick elements with 8 nodes and have convection/diffusion ability. To increase and improve the accuracy of the results, the mesh sensitivity analysis was done. Fig. 2 shows the element meshing and boundary conditions applied to the model.

The temperature of a point at the distance of 60 *mm* from the starting point and 10 *mm* from the weld line and 2.5 *mm* depth was recorded consistent with the experimental setup, and the temperature history was used for the model verification. The geometric location of this point has been shown in Fig. 3.
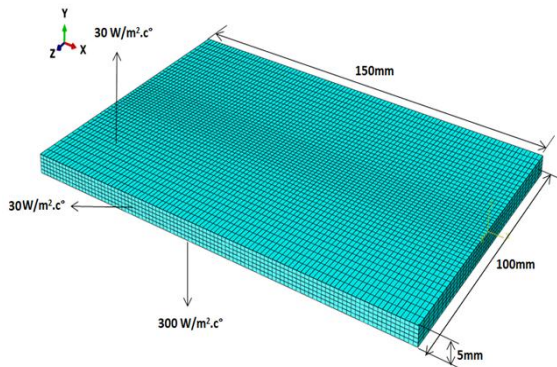
Fig.2
Mesh and boundary conditions of the work piece.
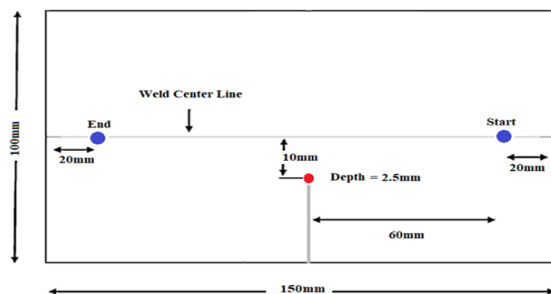
Fig.3
Thermocouple position in the experiment.

4   RESULTS AND DISCUSSION
4.1 Temperature distribution

Numerical simulation of the FSW process of AA6061-T6 was done using the current developed model and FORTRAN language coding in form of two DFLUX and USDFLD subroutines. Fig. 4 shows the comparison of the temperature history of the specified point for both numerical and experimental modes during 200 seconds.

Based on the comparison between experimental and numerical results, it was found that the current model, with the characteristic being high precision, can be potentially used to predict the temperature and its distribution in the

FSW process. The correct prediction of the temperature term in the FSW process leads to the correct prediction of stress, strain and material flow during the process. Fig. 5 shows the temperature distribution contours at the cross section of the welded work piece.

Based on the temperature distribution contour shown in Fig. 5, due to the presence of the shoulder on the top surface of the work piece and high frictional interaction in this area, the maximum process temperature has occurred at this location. By distancing from the shoulder and moving through the depth of the work piece, the existing thermal concentration is gradually reduced, and only in the pin areas and its margins, the distribution of temperature remains within the appropriate range. Considering the use of two surface and body heat fluxes which were based on developed relations, it was shown that in the case of using body flux consistent with the tool pin volume, the extent of the thermal regions around the pin can be reliably predicted.
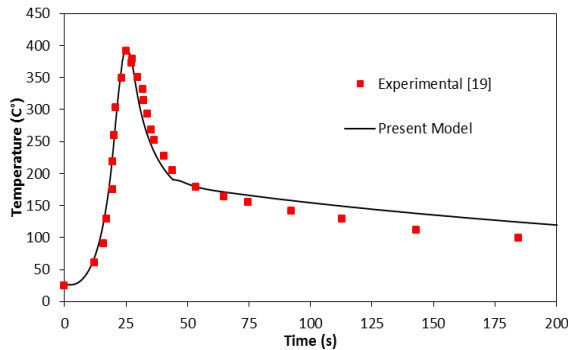
Fig.4
Comparison of numerical and experimental results.
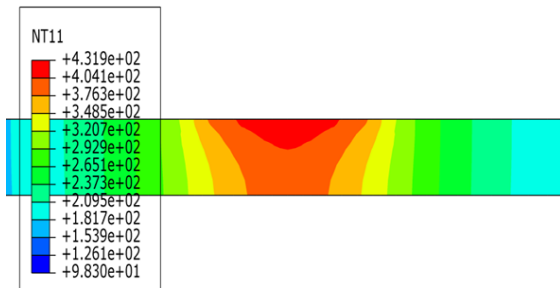
Fig.5
Temperature distribution at the welded cross section.

4.2 Residual stresses

After determining the temperature distribution obtained from new thermal model and validating the model, residual stresses in the FSW process were investigated. To evaluate the longitudinal and transverse residual stresses, an uncoupled thermo-mechanical model was used. To achieve this, after performing the FSW process described in the previous section, a cooling step with $600s$ duration was applied to the model. This step caused the work-piece temperature to become equal to ambient temperature. After that, a mechanical step was defined and the numerical results obtained from thermal steps were used as input to calculate the residual stresses. Longitudinal and transverse residual stresses of mid-plane of work-piece are shown in Fig. 6 and Fig. 7 respectively.

According to Fig. 6 and Fig. 7, the profiles of longitudinal and transverse residual stresses in welded cross-section are almost similar. The difference concerns the fact that the transverse residual stress is lower than the longitudinal one. As shown in the residual stress diagrams, a large portion of longitudinal and transverse residual stresses occur in the HAZ area because of sudden drop of effective plastic strain in this zone. It is important to note that the maximum positions of stresses are in compliance with findings of recent researches [21-23].

Based on the obtained results, it was found that a large portion of longitudinal residual stresses are close to the base metal yield stress and within the range of -60 to 100 MPa. This range of residual stress change in Al 6XXX has been reported in recent investigation [24]. Good agreement of residual stresses patterns and values implies the accuracy and correctness of presented model in prediction of residual stresses in the FSW process.
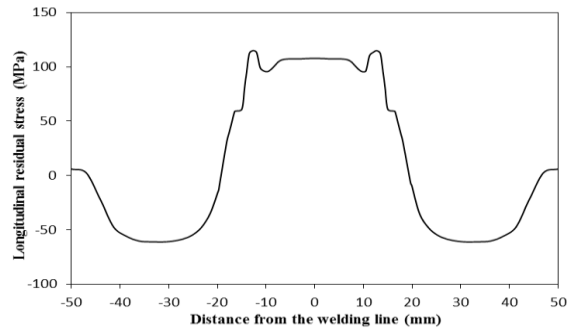
Fig.6
Longitudinal stress distribution at the welded cross-section.
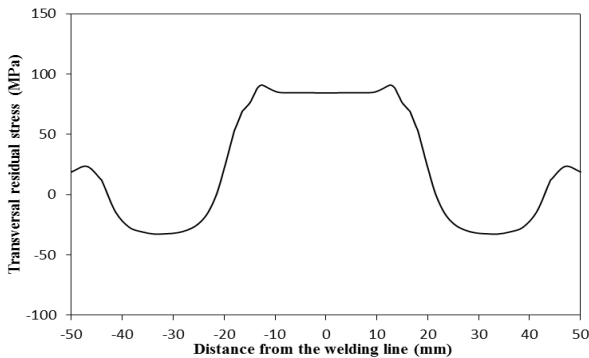
Fig.7
Transversal stress distribution at the welded cross-section.

5   CONCLUSIONS

In the current research, a modified analytical model independent from the coefficient of friction was developed based on the instantaneous dependent process variables in order to model the heat generation in the FSW process. Then, using the relationships obtained from the model, numerical simulation of the FSW process was performed employing the ABAQUS finite element code and the use of two subroutines DFLUX and USDFLD to predict the temperature distribution. Generally, the results of the current research are summarized as follows:

- Based on the relationship between the yield stress and the friction coefficient in the sliding interaction mode, the dependence of the final relations on the friction coefficient was eliminated, and the final relations were presented based on the tool rotational speed, tool geometry, and yield stress. This made it easy to simulate the FSW process.
- Comparing the results of the current model with the experimental results, it was found that the developed model, with the characteristic being high precision, can predict the temperature in the FSW process.
- By defining and using two surface and body heat fluxes to model the heat generation, a more precise heat distribution and prediction of temperature in the cross section of weld in FSW were obtained.

By using a body flux and applying it to the volumetric range of tool pin, distributing and applying heat through depth of work piece occur more effectively. It also makes it possible to examine the capability of pin geometry effect on the heat generation and temperature distribution in the cross section of weld.

REFERENCES

[1]   Thomas W., 1991, Friction stir welding, *International Patent Application*.
[2]   Mishra R.S., De P.S., Kumar N., 2014, *Friction Stir Welding and Processing: Science and Engineering*, Springer.
[3]   Ahmed M., 2017, Friction stir welding of similar and dissimilar AA7075 and AA5083, *Journal of Materials Processing Technology* **242**: 77-91.
[4]   Frigaard Q., Grong Q., Midling O., 2001, A process model for friction stir welding of age hardening aluminum alloys, *Metallurgical and Materials Transactions A* **32**(5): 1189-1200.

[5]   Chao Y.J., Qi X., Tang W., 2003, Heat transfer in friction stir welding—experimental and numerical studies, *Journal of Manufacturing Science and Engineering* **125**(1): 138-145.

[6]   Chen C., Kovacevic R., 2003, Finite element modeling of friction stir welding—thermal and thermomechanical analysis, *International Journal of Machine Tools and Manufacture* **43**(13): 1319-1326.

[7]   Khandkar M., Khan J.A., Reynolds A.P., 2003, Prediction of temperature distribution and thermal history during friction stir welding: input torque based model, *Science and Technology of Welding and Joining* **8**(3): 165-174.

[8]   Song M., Kovacevic R., 2003, Thermal modeling of friction stir welding in a moving coordinate system and its validation, *International Journal of Machine Tools and Manufacture* **43**(6): 605-615.

[9]   Schmidt H., Hattel J., Wert J., 2003, An analytical model for the heat generation in friction stir welding, *Modelling and Simulation in Materials Science and Engineering* **12**(1): 143.

[10]   Nandan R., 2007, Three-dimensional heat and material flow during friction stir welding of mild steel, *Acta Materialia* **55**(3): 883-895.

[11]   Schmidt H., Hattel J., 2005, Modelling heat flow around tool probe in friction stir welding, *Science and Technology of Welding and Joining* **10**(2): 176-186.

[12]   Riahi M., Nazari H., 2011, Analysis of transient temperature and residual thermal stresses in friction stir welding of aluminum alloy 6061-T6 via numerical simulation, *The International Journal of Advanced Manufacturing Technology* **55**(1-4): 143-152.

[13]   Russell M., Shercliff H., 1999, Analytical modelling of microstructure development in friction stir welding, *1st International Symposium on Friction Stir Welding*, Thousand Oaks, California.

[14]   Colegrove P.A., 2001, *3 Dimensional Flow and Thermal Modelling of the Friction Stir Welding Process*, University of Adelaide, Department of Mechanical Engineering.

[15]   Su H., 2015, Numerical modeling for the effect of pin profiles on thermal and material flow characteristics in friction stir welding, *Materials & Design* **77**: 114-125.

[16]   Amini S., Amiri M., Barani A., 2015, Investigation of the effect of tool geometry on friction stir welding of 5083-O aluminum alloy, *The International Journal of Advanced Manufacturing Technology* **76**(1-4): 255-261.

[17]   Meyghani B., 2017, Developing a finite element model for thermal analysis of friction stir welding by calculating temperature dependent friction coefficient, *2nd International Conference on Mechanical, Manufacturing and Process Plant Engineering*, Springer.

[18]   Hibbit H., Karlsson B., Sorensen E., 2012, ABAQUS user manual, version 6.12, Simulia, Providence, RI.

[19]   Aval H.J., Serajzadeh S., Kokabi A., 2011, Evolution of microstructures and mechanical properties in similar and dissimilar friction stir welding of AA5086 and AA6061, *Materials Science and Engineering A* **528**(28): 8071-8083.

[20]   Nandan R., 2006, Numerical modelling of 3D plastic flow and heat transfer during friction stir welding of stainless steel, *Science and Technology of Welding and Joining* **11**(5): 526-537.

[21]   Staron P., 2004, Residual stress in friction stir-welded Al sheets, *Physica B: Condensed Matter* **350**(1-3): E491-E493.

[22]   Khandkar M.Z.H., 2006, Predicting residual thermal stresses in friction stir welded metals, *Journal of Materials Processing Technology* **174**(1-3): 195-203.

[23]   Feng Z., 2007, Modelling of residual stresses and property distributions in friction stir welds of aluminium alloy 6061-T6, *Science and Technology of Welding and Joining* **12**(4): 348-356.

[24]   Dalle Donne C., Wegener J., Pyzalla A., Buslaps T., 2001, Investigation of residual stressesin friction stir welds, *Third International Symposium on Friction Stir Welding*, Kobe, Japan, TWI, Cambridge.